

# MULTI-OBJECTIVE OPTIMIZATION OF RF STRUCTURES\*

S. Smith<sup>†</sup>, M. Southerby<sup>‡</sup>, S. Setiniyaz, R. Apsimon, G. Burt  
Lancaster University, Cockcroft Institute, Lancaster, United Kingdom

## Abstract

In this work, we apply multi-objective optimization methods to single-cell cavity models generated using non-uniform rational basis splines (NURBS). This modeling method uses control points and a NURBS to generate the cavity geometry, which allows for greater flexibility in the shape, leading to improved performance. Using this approach and multi-objective genetic algorithms (MOGAs) we find the Pareto frontiers for the typical key quantities of interest (QoI) including peak fields, shunt impedance and the modified Poynting vector. Visualizing these results becomes increasingly more difficult as the number of objectives increases, therefore, in order to understand these frontiers, we provide several techniques for analyzing, visualizing and using multi-dimensional Pareto fronts specifically for RF cavity design.

## INTRODUCTION

Multi-objective optimization methods are employed when there are two or more conflicting objectives that must be optimized simultaneously, which is often the case in RF structure design. Mathematically these types of problems can be summarized as follows:

$$\begin{aligned} \min/\max f_m(x), \quad m = 1, 2, \dots, M, \\ \text{subject to } g_j(x) \geq 0, j = 1, 2, \dots, J, \\ x_{ilb} \leq x_i \leq x_{iub}, \quad i = 1, 2, \dots, n \end{aligned} \quad (1)$$

Where  $f_m$  are the objectives,  $g_j$  are the constraints, and  $x_i$  are the upper and lower bounds of the input parameters. A unique, optimal solution to these problems does not exist, and instead a set is found that defines the trade-off between the objectives. This is shown in Fig. 1 for a 2D case where the two objectives  $f_1$  and  $f_2$  are to be minimized. The set of solutions that are not dominated by any other feasible points are called Pareto optimal points and when mapped to the objective space, they make up the Pareto frontier.

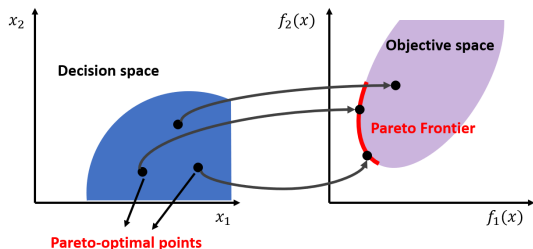


Figure 1: Pareto-optimal solutions in 2D.

\* Supported by Research Grant: ST/P002056/1

<sup>†</sup> s.smith26@lancaster.ac.uk

<sup>‡</sup> m.southerby@lancaster.ac.uk

## APPLYING MOGAS TO RF CAVITIES

To explore these methods, a generic X-band (12 GHz),  $\beta = 1, 2\pi/3$  travelling wave cavity has been optimized, with an assumed desired group velocity ( $v_g$ ) of 1%. The objectives used for the optimization were: maximizing the shunt impedance per unit length ( $Z$ ), whilst minimizing the peak normalized electric field, magnetic field and modified Poynting vector ( $E_{peak}/E_{acc}$ ,  $B_{peak}/E_{acc}$  and  $\sqrt{S_c}/E_{acc}$ , respectively [1]). The constraints on the optimization problem were that the fundamental accelerating mode frequency had to be kept constant and that the nose cone of the optimized geometry could be feasibly manufactured.

## Modeling Methods

Two types of cavity modeling methods were considered, one using standard shapes such as circular radii and angles to define the nose cone geometry and the other a model using NURBS and control points to generate the geometry allowing for much greater control of the nose cone shape [2]. The two methods and geometries are shown in Fig. 2.

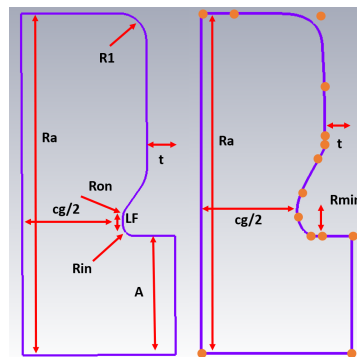


Figure 2: Standard parameters vs. spline geometry.

## OPTIMIZATION

The MOGA's used for the optimization were the Fast Non-dominated Sorting Genetic Algorithm (NSGA-II) [3], and the Archive-Based Micro Genetic Algorithm (AMGA), although other algorithms were explored including the Neighborhood Cultivation Genetic Algorithm (NCGA). The optimizations were performed using ISIGHT [4] with CST MWS [5] used to calculate the cavity fields.

## Algorithms

The initial population size was chosen based on the number of input parameters, typically using values of 60-100 individuals. The cavity resonant frequency was handled using a constraint method with  $\epsilon = 40$  MHz and to handle

the requirement of the group velocity a number of options were considered:

1. Having  $v_g$  as an objective with an appropriate choice of the aperture radius upper and lower bounds.
2. Having  $v_g$  as a constraint, similar to the frequency.
3. Choosing a fixed value of the aperture radius based on estimates and allowing  $v_g$  to vary between constrained bounds.
4. Having  $v_g$  as both an objective and a constraint.

Table 1: Algorithm Parameters.

Parameter	Value
Population Size	60
Crossover Probability	0.9
Crossover Distribution Index	9
Mutation Distribution Index	18

The constraint placed on  $v_g$  was  $\pm 0.05\%$  of  $c$  and the algorithm parameters were kept constant for the various runs, as shown in Table 1. The results of an investigation into the algorithms and options for handling  $v_g$  are shown in Fig. 3. By fixing the aperture radius, convergence to a similar Pareto front can be significantly faster as shown by the 6th and 7th runs, although this limits the ability of the algorithm to maximize  $Z$  at higher values of  $E_{peak}/E_{acc}$  as  $Z$  is highly dependent on the aperture size.

The best results were obtained by estimating a value of the aperture radius, allowing the algorithm to search within  $\pm 1\text{mm}$  and having  $v_g$  as an objective and a constraint. As shown in the last run, after 10k evaluations it had already outperformed the other methods in terms of the highest values of  $Z$  for the same  $v_g$  bounds.

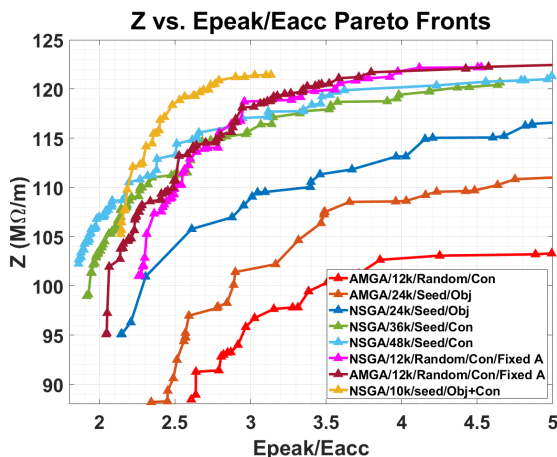


Figure 3:  $Z$  vs.  $E_{peak}/E_{acc}$  Pareto Fronts.

An example of a 2D Pareto front for  $E_{peak}/E_{acc}$  vs.  $\sqrt{S_c}/E_{acc}$  is shown in Fig. 4. By binning  $Z$  and finding

the Pareto front for each bin, information about the optimal geometry can be obtained. The lowest values of  $E_{peak}/E_{acc}$  come at the expense of a much lower  $Z$  and a higher value of  $\sqrt{S_c}/E_{acc}$ , while the highest values of  $Z$  increase both peak fields. In the centre though, for a modest increase in  $E_{peak}/E_{acc}$ ,  $Z$  can be increased significantly whilst also decreasing  $\sqrt{S_c}/E_{acc}$ .

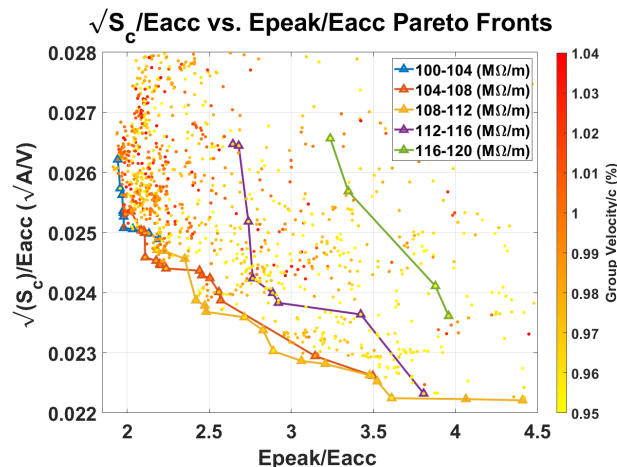


Figure 4:  $\sqrt{S_c}/E_{acc}$  vs.  $E_{peak}/E_{acc}$  Pareto Fronts.

## VISUALIZATION METHODS

Once the MOGA has converged to a Pareto frontier in  $N$ -dimensional objective space, visualisation techniques must be implemented to explore the trade-off between objectives.

In order to visualise a design space for a multi-objective problem, various methods have been developed. Whilst many methods do provide ways to observe the range and structure of an objective space, some do not readily allow a user to optimise a single cell as they use often use dimensionality reduction (DR) or goal functions to aid visualisation, potentially losing individual objective trade-offs. Some common examples of DR are Projection [6] and 3D Radial Coordinate Visualisation (3dRadVis) [7]. These methods work by constricting the objective space to a refined subspace which ideally allows the user to retain all the relevant information, and loses information that is not useful.

Not all data sets allow for DR to retain all useful information. As an example, a circular particle distribution with Gaussian particle density can be reduced in dimension ( $x, y \rightarrow r$ ) with no loss of information, as the data set has rotation symmetry. If instead the particle distribution is elliptical, performing DR ( $x, y \rightarrow r$ ) will lose information regarding the rotation angle of the ellipse [9]. As a result, combining  $E_{peak}/E_{acc}$  and  $\sqrt{S_c}/E_{acc}$  into one objective (as is done in Projection) will enable good points to be selected, however all information of individual objectives is forfeit. The aim is to provide a self-consistent method that can be repeated for all single cell design studies.

Decision maps (DMs) are an effective way of displaying three objectives. DMs display bi-objective Pareto front

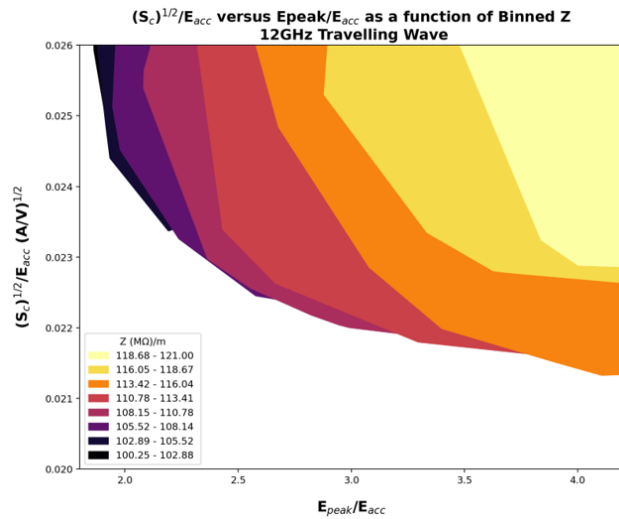


Figure 5: DM showing the Pareto front for  $E_{peak}/E_{acc}$  versus  $\sqrt{S_c}/E_{acc}$  as a function of  $Z$ .

slices as a function of a third, and recently, more objectives can be visualised via Interactive DMs [8]. Figure 5 displays three objectives in the form of a DM. The Pareto front for two objectives is shown as a function of a third dimension, which is shown using colour. Figure 5 could incorporate an additional objective by plotting the front as a line with different line style. As a result it would be possible to display the Pareto front of  $E_{peak}/E_{acc}$  versus  $\sqrt{S_c}/E_{acc}$  at a particular  $Z$  and surface magnetic field, for example.

All five objectives can be shown on a single plot if colour and point size variables are introduced (in fact, six dimensions are possible if point shape is also used). Figure 6 shows five objectives for Pareto optimal points only. This is not massively useful as when three spatial dimensions are used, clarity is lost when projecting the plot onto a 2D plane.

Another method that can display all objectives on one plot without utilising DR is the parallel coordinate plot. Parallel coordinate plots display a solution as a line crossing equally spaced axis representing each objective. Figure 7 shows a parallel coordinate plot where the objectives are temperatures at different times in a geographic example [10]. The plot is shown twice with different axis scaling. The production of the parallel coordinate plot possess four degrees of freedom, such as the objective axis order, and the scale of each axis. Parallel coordinate plots are a powerful way to display the objective space and display trade-offs that are not clear from other visualisation techniques such as the bubble scatter plot. These will be explored in future work.

## CONCLUSION

Multi-objective genetic algorithms have been applied to a 12 GHz TW single cell cavity design space with the intent to maximise/minimise the key qualities of interest. New modeling methods have also been employed that allow a higher shunt impedance to be realized for the same peak fields. An

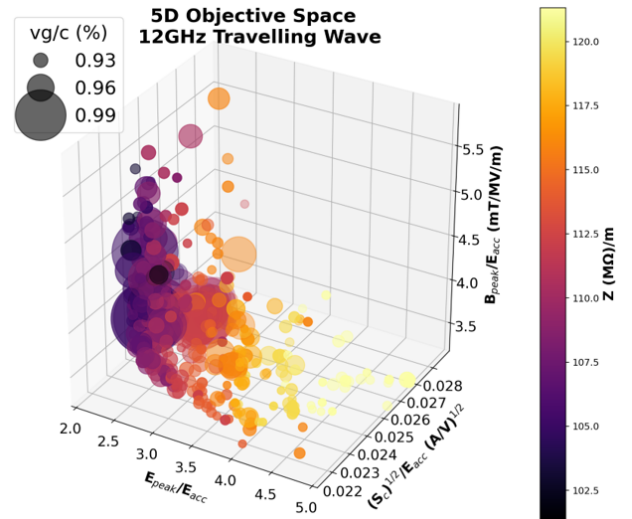


Figure 6: 5D bubble scatter plot showing all Pareto optimal solutions for all objectives.

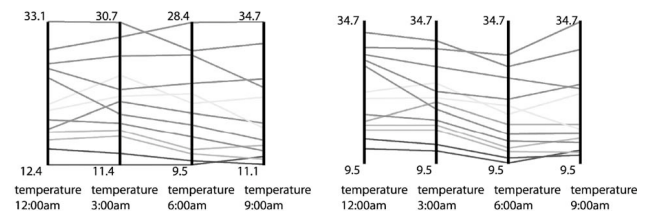


Figure 7: Parallel Coordinate Plot.

optimum method for handling  $v_g$  has been identified along with an appropriate choice of algorithm for fast convergence. A variety of visualisation techniques have then been introduced to explore the N-dimensional Pareto fronts and better understand the trade-offs between the objectives.

## REFERENCES

- [1] A. Grudiev, S. Calatroni, and W. Wuensch, "New local field quantity describing the high gradient limit of accelerating structures", *Physical Review Special Topics-Accelerators and Beams*, vol. 12, no. 10, p. 102001, 2009. doi:10.1103/PhysRevSTAB.12.102001
- [2] M. H. Nasr and S. G. Tantawi, "New Geometrical-Optimization Approach using Splines for Enhanced Accelerator Cavities' Performance", in *Proc. 9th Int. Particle Accelerator Conf. (IPAC'18)*, Vancouver, Canada, Apr.-May 2018, pp. 4395-4397. doi:10.18429/JACoW-IPAC2018-THPMK049
- [3] K. Deb, A. Pratap, S. Agarwal, and T. Meyarivan, "A fast and elitist multiobjective genetic algorithm: NSGA-II", *IEEE Transactions on Evolutionary Computation*, vol. 6, no. 2, pp. 182-197, Apr. 2002. doi:10.1109/4235.996017
- [4] ISIGHT & THE SIMULIA EXECUTION ENGINE, <https://www.3ds.com/products-services/simulia/products/isight-simulia-execution-engine/>.
- [5] CST STUDIO SUITE, <https://www.3ds.com/products-services/simulia/products/cst-studio-suite/>.

- [6] T. Tušar and B. Filipič, “Visualization of Pareto Front Approximations in Evolutionary Multiobjective Optimization: A Critical Review and the Prosection Method”, *IEEE Transactions on Evolutionary Computation*, vol. 19, no. 2, pp. 225-245, Apr. 2015. doi:10.1109/TEVC.2014.2313407
- [7] A. Ibrahim, S. Rahnamayan, M. V. Martin, and K. Deb, “3D-RadVis: Visualization of Pareto front in many-objective optimization”, presented at *IEEE Congress on Evolutionary Computation (CEC)*, Vancouver, Canada, Jul. 2016, pp. 736–745.
- [8] A. V. Lotov, V. A. Bushenkov, and G. K. Kamenev, *Interactive decision maps: Approximation and visualization of Pareto frontier*, NY, USA: Springer US, 2013.
- [9] K. Deb and D. Saxena, “Searching for Pareto-optimal solutions through dimensionality reduction for certain large-dimensional multi-objective optimization problems”, in *Proceedings of the World Congress on Computational Intelligence*, Kunming, China, Aug. 2006, pp. 3352–3360.
- [10] R. M. Edsall, “The parallel coordinate plot in action: design and use for geographic visualization”, *Computational Statistics & Data Analysis*, vol. 43, no. 4, pp. 605-619, 2003. doi:10.1016/S0167-9473(02)00295-5